

Theoretical determination of the adsorption geometry of Na on the Si(001) surface

P. Gravila and P. F. Meier

Physics Institute, University of Zurich, CH-8057 Zurich, Switzerland

(Received 19 June 1998)

Ab initio total-energy calculations for Na on the Si(001) 2×1 surface at coverages ranging from one-fourth to one monolayer were performed using the density-functional method with a plane-wave basis set and a slab with a 2×2 surface cell. The results of these electronic structure calculations are discussed and compared with other theoretical and experimental findings. At the highest coverage of one monolayer, we obtained the lowest surface energy for the double-layer model with combined occupation of the hollow and pedestal sites. For lower coverages, the structures are more complicated, as the hollow site becomes unstable and adsorption at the cave and the pedestal site is preferred. In particular, for half a monolayer a distinct larger adsorption energy is obtained for the combination of cave and pedestal sites. [S0163-1829(98)08348-9]

I. INTRODUCTION

Although alkali-metal (AM) adsorption on the Si(001) surface has been a topic of great interest due to its scientific and technological importance, some aspects of this system remain controversial. A very early model for alkali-metal adsorption on Si(001) proposed by Levine¹ assumes that AM atoms form a linear chain on top of the Si dimers, with a saturation coverage of one half of a monolayer. Since the ML coverage has been defined differently, we specify our definition: 1 ML = 6.78×10^{14} adsorbates/cm², i.e., two adsorbates per Si dimer or per Si 2×1 surface cell. On the Si(001) surface, several symmetric sites are possible candidates for AM adsorption, and there is no agreement on which sites really are occupied for a given coverage.

Mangat *et al.*² claimed, based on experimental and theoretical (cluster) considerations, that the AM adsorption is taking place only at the cave site, also supporting a maximal coverage of $\frac{1}{2}$ ML. On the other hand, Enta, Suzuki, and Kono³ (using angle-resolved photoemission) and Abukawa and Kono⁴ (using photoelectron diffraction) proposed a double-layer structure. In this model the AM adsorbates are located above the third layer of Si atoms, in the pedestal and hollow (or valley bridge) sites, with coverages up to 1 ML. Most theoretical calculations, especially *ab initio* pseudopotential calculations, support the double-layer model (Batra, Refs. 5–7, and others).

Zhang, Chan, and Ho⁷ claimed that the saturation coverage is 1 ML, with adsorbates in pedestal and hollow sites, while at $\frac{1}{2}$ ML the adsorption site is the hollow site. This can be expected for calculations with a surface cell of 2×1 only. The situation may change, however, if larger supercells are considered.

Ko, Chang and Yi⁸ investigated the adsorption in a 2×2 and a 4×1 surface supercell. With the 2×2 surface cell they found that the adsorption at the cave site is slightly more favorable than at the hollow site; however, they found an even lower energy in a 4×1 reconstruction where only hollow sites are occupied at low coverages. Kobayashi *et al.*⁹ used, in addition to the 2×1 calculations, a 2×3 surface cell. They used a cutoff energy of 6.25 Ry with four k points for the 2×3 cell and 32 k points for the 2×1 cell. They studied

the adsorption geometries at $\frac{1}{3}$, $\frac{1}{2}$, $\frac{5}{6}$, and 1 ML coverages, and found that the hollow site is always preferred over the cave site, in contradiction to their previous results¹⁰ which were obtained without the use of partial core corrections for the alkali-metal atoms. We will compare our results to those of Refs. 8 and 9 in Sec. IV.

In this work we present results of extended first-principles calculations for the total energy of Na adsorption at the various sites on the Si(001) surface for four different coverages. The density-functional method^{11–13} with a plane-wave basis set is used. To account for periodic boundary conditions, a slab model was employed. The Si(001) surface has a 2×1 reconstruction due to the pairing of the topmost Si atoms. We used two identical 2×1 cells resulting in a 2×2 surface cell as the substrate for Na adsorption, in order to study coverages lower than half of a monolayer, and to allow more reconstruction possibilities for higher coverages. Our results propose a solution to the contradiction that those authors who support the double-layer model usually find the hollow (together with the pedestal) site to be stable, while others who are supporting only one adsorption site favor the cave (and not the hollow) site.

We find that the cave site is stable for small coverages, but for higher coverages we observe that the cave site Na adsorbates migrate into the hollow sites. Small coverages are better modeled in cluster calculations, while calculations, using periodic boundary conditions do not allow the investigation of arbitrarily low coverages. A 2×1 surface cell, e.g., only permits the study of $\frac{1}{2}$ or 1 ML.

This paper is organized in the following way. In Sec. II we present the theoretical method and calculational details. The results for the clean surface and the Na-Si surfaces at different coverages are given in Sec. III. Section IV contains additional discussions and a summary.

II. METHOD AND CALCULATIONAL DETAILS

All calculations were carried out using the molecular-dynamics density-functional program *fhi96md* developed by Scheffler and co-workers.^{14,15} It is known¹³ that the molecular dynamics method—indirect minimization of the energy—needs a longer time from “nearly converged” to “con-

verged” solutions than the method of direct minimization (eventually using a conjugate gradient method). But when the ions are simultaneously moved this method proves to be a valuable and efficient tool. We used fully separable *ab initio* pseudopotentials after Kleinman and Bylander,¹⁶ and non-linear core corrections for the pseudopotential of Na were employed.¹⁷ All calculations were done in the local-density approximation with the exchange-correlation potential taken from the results of Ceperley and Alder¹⁸ in the Perdew and Zunger parametrization.¹⁹

We chose a slab model of eight Si layers and the equivalent of 12 layers of vacuum. To diminish nonphysical interactions between the two surfaces through the vacuum, we saturated the silicon bonds at the bottom of the slab with hydrogen atoms. Also, the method developed by Neugebauer and Scheffler²⁰ of introducing a planar dipole layer in the middle of the vacuum region was employed. The dipole strength is adjusted to compensate for the adsorbate-induced dipole. In this way, without losing accuracy, the number of vacuum layers has not to be increased, keeping the vertical dimension of the slab supercell to reasonable values.

Taking into account that the surface may have metallic character we used for the calculations a grid of 16 k points in the surface Brillouin Zone. Exploratory calculations were initially made with fewer k points. Two different methods were applied for setting up the k -point grid: one is described in Refs. 21–23, the other was used in Ref. 24.

The calculations were done mainly at a cutoff energy of 8 Ry. Several tests were performed with cutoff energies up to 14 Ry. They showed that, although the total energies still decreased with increasing E_{cutoff} , the energy differences and the bond length do not vary significantly for cutoff energies above 8 Ry.

III. RESULTS

A. Clean Si surface

First, the relaxation of the clean Si(001) surface was investigated in a 2×2 cell. The positions of the Si atoms of the third and deeper levels were fixed at their bulk sites, while those of the eight Si atoms of the two top layers were optimized.

The lowest energy was found for a 2×2 reconstruction with alternating buckled dimers. This reconstruction is practically degenerate in energy with the 2×1 surface with non-alternating buckled dimers. Our calculated Si-Si dimer distance for the clean surface (using 14-Ry cutoff energy) is $D = 2.29$ Å. Photoemission extended x-ray-adsorption fine-structure measurements (Refs. 2 and 25) yield $D = 2.20 \pm 0.04$ Å, while classical low energy electron-diffractions data^{26,27} give $D = 2.40 \pm 0.10$ Å.

B. Adsorption sites and procedures

The four sites for Na adsorption investigated are shown schematically in Fig. 1. The pedestal (p) and the hollow (h) sites are located above the third layer of Si, and the bridge (b) and cave (c) sites above the fourth Si layer (note that the hollow site is also called the valley-bridge site). For convenience, we call the open region above the third and fourth Si

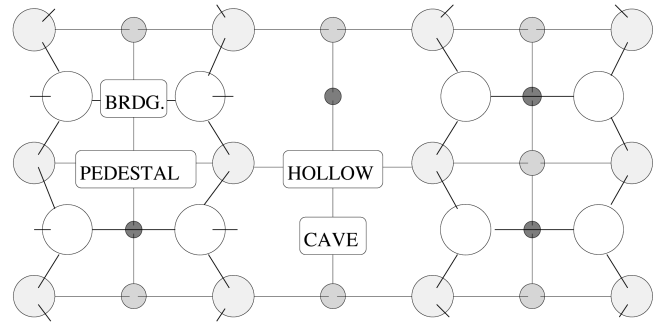


FIG. 1. Schematic top view of the Na/Si(001) surface. Adsorption sites for Na: the pedestal (p) and the hollow (h) (valley bridge) sites are located above the third layer of Si, the bridge (b) and cave (c) sites above the fourth Si layer.

layers the “trough.” It is directed along $[110]$. Adsorption at each of these four sites in various combinations was studied for coverages of $\frac{1}{4}$, $\frac{1}{2}$, $\frac{3}{4}$, and 1 ML. As initial positions the Na atoms were placed above the corresponding adsorption site, and the substrate atoms were arranged according to the relaxed clean Si surface but without the tilted dimers. The total energy was then minimized by relaxing the positions of the Na and the eight Si atoms of the two top layers.

C. $\frac{1}{4}$ -ML coverage

In the initial stages of the energy optimization the Na approaches the surface with a simultaneous relaxation of the substrate atoms. For adsorption at the bridge site and the hollow site, quasistationary energy minima with energies of E_b and E_h are obtained, which last for several iteration steps. However then these sites turn out to be unstable and the energy is further reduced when the Na eventually moves from the b site toward the pedestal site and from the h site toward the cave site, respectively. We did not find any significant potential barrier between the h and c sites, nor between b and p . The adsorption energies per adatom and the geometries of the equilibrium surfaces are given in Table I (also see Fig. 2).

In Fig. 2 we also depict the adsorption energy per adatom. As the reference energy we used the sum between the total energy of a clean Si(001) system and the energies of free Na atoms. The latter were determined using a separate *ab initio* calculation with the same pseudopotential. The Na atoms were put in a bulk configuration but with a very large lattice constant (about 15 Å) in order to approximate free atoms and at the same time maintain periodic boundary conditions. The spin-polarization energy for Na (0.32 eV) is included.

Note that in contrast to the starting positions, the energetically most favorable reconstruction for adsorption on the pedestal site is not symmetric (see Fig. 3). The Si dimers are tilted, alternating by about 0.7 Å and the distance $d_{\text{Na-Si}}$ is 2.9 Å for the two upmost Si atoms and 3.2 Å for the other two Si atoms which form the substrate at the pedestal site (see Table I). A symmetric reconstruction for the p site appears to be higher in energy than the cave site. The pedestal site with strongly tilted Si-Si dimers and the cave site are both stable, being separated by a potential barrier which we calculated to be 0.5 to 1 eV high.

TABLE I. Converged total energy and geometry details for various coverages and site occupancies. Energies in parentheses indicate unstable adsorption sites. The numbers for the Na-Si bond length marked with an asterisk denote the distances from Na atoms in the hollow sites to the Si atoms in the second layer. h denotes the height above the surface (i.e., from the middle of the nearest Si dimer).

Cov.	site Si(001)	ads. energy (eV)	Si-Si dimers (Å)		h (Å)
			2.29	Na-Si bonds (Å)	
$\frac{1}{4}$	p	2.26	2.31	2.9/3.2	2.0
$\frac{1}{4}$	c	2.19	2.38/2.24	2.8	1.0
$\frac{1}{4}$	h	(1.92)	2.34	3.1*	1.2
$\frac{1}{2}$	cp	2.11	2.44/2.29		1.0/2.0
$\frac{1}{2}$	hh	1.85	2.46		1.1
$\frac{1}{2}$	pp	1.81	2.38		1.9
$\frac{1}{2}$	hp -diag	(1.88)			
$\frac{1}{2}$	hp -line	(1.84)			
$\frac{1}{2}$	cc	(1.80)			
$\frac{3}{4}$	hhp	2.00	2.56		0.9/1.8
$\frac{3}{4}$	cpp	1.97	2.42/2.46		1.1/1.9
$\frac{3}{4}$	hpp	(1.94)	2.53		1.0/1.8
1	$h-h-p-p$	2.04	2.64		1.0/1.8

Another observation is that the adatom in the h site is nearer to the two atoms from the second layer than to the four top Si atoms which form the h site. The position of the Na atom in the h site is almost degenerate in energy for small moves in the x - y plane (large vibrational amplitude).

D. $\frac{1}{2}$ -ML coverage

For a coverage of half a monolayer (i.e., one Na atom per one Si dimer), we can consider adsorption at pairs of the four sites, i.e., at ten positions, since we have a 2×2 surface cell. This is in marked contrast to investigations with a 2×1 cell where only the four symmetric pairs (b - b , p - p , c - c , and h - h) are accessible. In our calculations, c - p adsorption with the occupation of every second cave site simultaneously with that of a every second pedestal site is energetically most favorable. An inspection of Fig. 2 shows that the energies for adsorption of Na at the same sites are distinctively higher.

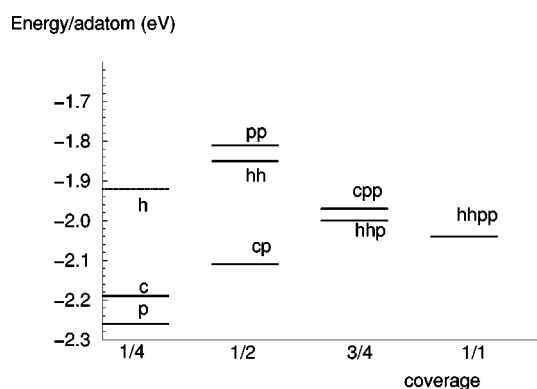


FIG. 2. Converged total adsorption energy per adatom for various sites at different coverages.

The converged total energy for the h - h adsorption is higher than for c - p but lower than for p - p . If all pedestal sites along the row are occupied, the previously observed tilt of the Si-Si dimers at the surface is reversed; the substrate restores a strict 2×1 periodicity that will be kept up to full coverage. Without the tilted dimers, the pedestal sites occupancy (p - p) turns out to be less favorable than the other stable sites, as previously mentioned.

The cave-cave adsorption is unstable: The Na atoms in a trough “prefer” the hollow-hollow sites. This is in contrast to the case of a smaller coverage, where the hollow site is unstable and every second cave site is preferred. This is an example of the general rule we have also found to hold for

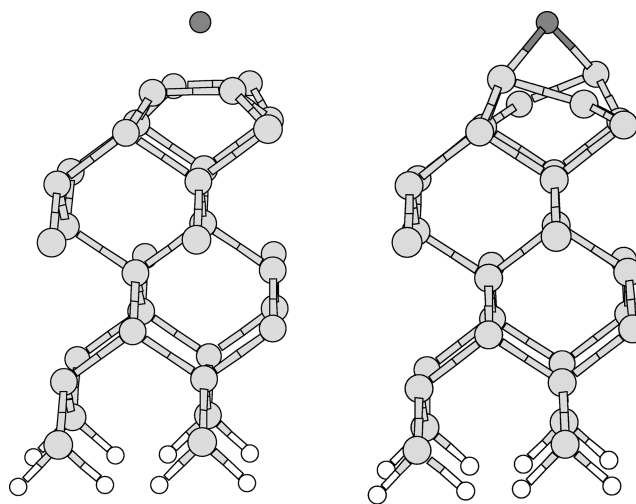


FIG. 3. Pedestal site reconstructions at a coverage of $\frac{1}{4}$. A symmetric reconstruction is shown on the left. On the right, the energetically more favorable (by about 0.3 eV) converged reconstruction with alternating tilted dimers is depicted.

higher coverages: the c site is stable when the neighboring c sites are empty. But if the number of Na atoms in the trough along the $[110]$ direction increases, the tendency of the adsorbates to move to the cave sites is reversed, and, instead, the hollow site with the neighboring h sites also occupied is more stable. It should be emphasized that these findings do not depend on an interpretation of the energy differences alone, but are also reflected in the outcome of the geometric optimizations using the Hellman-Feynman forces.

In Ref. 7, the possibility of subsurface adsorption was investigated. Similar to these results, we did not find any stable subsurface adsorptions.

E. Higher coverages

For a coverage of $\frac{3}{4}$ ML, we have found two possible adsorption geometries that are very close in energy: c - p - p and h - h - p occupations. Other choices turn out to be unstable, as expected from the above rules: c - c - p transforms into h - h - p and h - p - p goes into c - p - p .

For one full monolayer we found only one stable adsorption geometry, h - h - p - p , a double-layer pattern with the adatoms situated above the third Si layer. This adsorption keeps the 2×1 periodicity of the clean Si(001) surface, with the Si dimers stretched 2.64 Å apart.

IV. DISCUSSION AND SUMMARY

We have performed *ab initio* total-energy calculations and geometry optimizations using Hellman-Feynman forces for a clean Si(001) surface with and without Na adsorbates. For a coverage of one full monolayer we found a double-layer structure of 2×1 periodicity with the occupation of all hollow and pedestal sites for a maximum coverage of 1 ML. This is in agreement with most previous theoretical results. In particular, the calculated adsorption energy per Na atom of 2.04 eV and the Si-Si dimer distance of 2.64 Å agree with the results of Ref. 8 (2.06 eV and 2.63 Å).

For a coverage of $\frac{1}{2}$ ML of Na adsorbates, we found that the combined pedestal-cave adsorption is energetically more favorable than all situations where adsorption was considered only at the same sites. It lies deeper in energy by 0.26 eV than the hollow-hollow site. For this coverage, Ko, Chang, and Yi⁸ considered only adsorptions at two equivalent sites in the 2×2 surface cell, thus missing exactly the configuration that yields the lowest energy. For the h - h adsorption, our values for the adsorption energy (1.85 eV) and the Si-Si dimer distance (2.46 Å) agree with the results of Ref. 8 (1.94 eV and 2.46 Å). For coverages of $\frac{1}{4}$ ML we found that both pedestal and cave sites are stable and rather close in energy.

Ko, Chang, and Yi⁸ investigated the adsorption in both 2×2 and 4×1 surface supercells. At $\frac{1}{4}$ coverage, using the 2×2 surface cell, for the cave site they obtained a larger adsorption energy than for the pedestal and hollow sites. They noted the tilted dimers for the $p(2\times 2)$ reconstruction, and found that the tilting reduces the energy by about 0.1 eV. Our results indicate a higher-energy gain due to the tilting (0.3 eV), with the consequence that the pedestal site appears

slightly more favorable (by about 0.07 eV) than the cave site. However, the potential barrier between the stable pedestal and cave sites is much higher (0.5–1 eV) than the difference in energy between them (less than 0.1 eV) and we expect that from the beginning of the adsorption process we will have adsorbates, in comparable numbers, in both sites.

Ko, Chang, and Yi,⁸ using a 4×1 surface cell, found even more favorable adsorption at the hollow site. But, due to the periodic boundary conditions, occupation of a hollow site in a 4×1 (or 2×1) geometry necessarily implies that all hollow sites along a trough are also occupied. In this case, there is no contradiction to the rule we found for the occupation of the sites along the trough. The hollow sites are indeed the most energetically favorable since the cave sites in a 4×1 reconstruction have to be unstable because they cannot have empty neighboring cave sites along the same trough. So, for a coverage of $\frac{1}{4}$ ML, Ko, Chang, and Yi⁸ found a reconstruction with one row (along the trough) fully packed with adsorbates while periodically alternating with neighboring empty rows.

We expect that, besides the 4×1 structures (if present), there are other reconstructions employing pedestal and cave sites that are contributing to the structure of the surface even at low coverages. The model of adsorption that our results imply suggests the following way to adsorb the Na atoms starting with small coverage and ending with a full ML: we predict that, as the AM layer starts growing, the Na atoms are adsorbed at cave and pedestal sites with almost equal probability. This continues smoothly until the coverage approaches $\frac{1}{2}$ ML of a ML. For $\frac{1}{2}$ ML we do not agree with the most frequently used model with AM atoms occupying all hollow sites while pedestal sites are still empty. Then, as the population of AM's in the troughs increases, the Na atoms previously situated in the cave sites undergo a transition by moving into the hollow sites. The AM's in the pedestal sites remain there, and the adsorption can go on until a coverage of 1 ML is reached, and by then every hollow and every pedestal site will be occupied. According to these results, the critical coverage is 1 ML for Na adsorption on Si(001).

The investigation of other reconstructions for the complicated adsorption geometries at small coverages probably requires a more extended frame than our 2×2 surface cell. It is possible, by example, that a more favorable reconstruction of the hollow site at low coverage along the trough can be found in a 4×2 frame, thus contradicting our affirmations regarding adsorbate movements between cave and hollow sites. The argument of Ref. 8 can be viewed as a hint in this direction. However, at this stage, we reject the possibility of drawing conclusions based on the 4×1 calculations because they can only simulate situations where all hollow sites in a trough are simultaneously occupied.

Kobayashi *et al.*⁹ argued for the importance of using non-linear core corrections (NLCC's) in the alkali-metal pseudopotential. The use of NLCC's resulted in a higher Na-Si bond length and in a favorization of the hollow sites over the cave sites. While we also observed this effect of NLCC's on the bond lengths, we found that NLCC's do not change the preference for the cave site in the low coverage regime. For their calculations Kobayashi *et al.*⁹ used a 2×3 surface cell as well as a 2×1 cell. They studied *in extenso* the adsorption

geometries at $\frac{1}{3}$ -, $\frac{1}{2}$ -, $\frac{5}{6}$ -, and 1-ML coverages. At the $\frac{1}{3}$ coverage they have a situation with two adsorbates occupying two out of the three possible hollow sites in the trough of the 2×3 surface cell. They do not give results for the lowest coverage of $\frac{1}{6}$ (i.e., an almost isolated Na atom in the trough) which would be interesting for our considerations. The preference for the hollow sites they calculated at $\frac{2}{3}$ occupancy of

the trough (corresponding to their $\frac{1}{3}$ coverage situation) is not in contradiction to our results.

ACKNOWLEDGMENTS

This work was partially supported by the Swiss National Science Foundation. We thank J. Osterwalder, T. Greber, and E.P. Stoll for constructive discussions.

-
- ¹J. D. Levine, Surf. Sci. **34**, 90 (1973).
²P. S. Mangat, P. Soukiassian, K. M. Schirm, L. Spiess, S. P. Tang, A. J. Freeman, Z. Hurych, and B. Delley, Phys. Rev. B **47**, 16 311 (1993).
³Y. Enta, S. Suzuki, and S. Kono, Surf. Sci. **242**, 277 (1991).
⁴T. Abukawa and S. Kono, Phys. Rev. B **37**, 9097 (1988).
⁵I. P. Batra, Phys. Rev. B **43**, 12 322 (1991).
⁶Y. Morikawa, K. Kobayashi, K. Terakura, and S. Blügel, Phys. Rev. B **44**, 3459 (1991).
⁷B. L. Zhang, C. T. Chan, and K. M. Ho, Phys. Rev. B **44**, 8210 (1991).
⁸Y.-J. Ko, K. J. Chang, and J.-Y. Yi, Phys. Rev. B **51**, 4329 (1995).
⁹K. Kobayashi, Y. Morikawa, K. Terakura, and S. Blügel, Phys. Rev. B **45**, 3469 (1992).
¹⁰K. Kobayashi, S. Blügel, H. Ishida, and K. Terakura, Surf. Sci. **242**, 349 (1991).
¹¹P. Hohenberg and W. Kohn, Phys. Rev. **136**, B864 (1964).
¹²W. Kohn and L. J. Sham, Phys. Rev. **140**, A1133 (1965).
¹³M. C. Payne, M. P. Teter, D. C. Allan, T. A. Arias, and J. D. Joannopoulos, Rev. Mod. Phys. **64**, 1045 (1992).
¹⁴R. Stumpf and M. Scheffler, Phys. Rev. B **40**, 12 255 (1989).
¹⁵M. Bockstedte, A. Kley, J. Neugebauer, and M. Scheffler, Comput. Phys. Commun. **107**, 187 (1997).
¹⁶L. Kleinman and D. M. Bylander, Phys. Rev. Lett. **48**, 1425 (1982).
¹⁷S. G. Louie, S. Froyen, and M. L. Cohen, Phys. Rev. B **26**, 1738 (1982).
¹⁸D. M. Ceperley and B. J. Alder, Phys. Rev. Lett. **45**, 566 (1980).
¹⁹J. P. Perdew and A. Zunger, Phys. Rev. B **23**, 5048 (1981).
²⁰J. Neugebauer and M. Scheffler, Phys. Rev. B **46**, 16 067 (1992).
²¹H. J. Monkhorst and J. D. Pack, Phys. Rev. B **13**, 5188 (1973).
²²S. Froyen, Phys. Rev. B **39**, 3168 (1989).
²³D. J. Chadi and M. L. Cohen, Phys. Rev. B **8**, 5747 (1973).
²⁴A. Ramstad, G. Brocks, and P. J. Kelly, Phys. Rev. B **51**, 14 504 (1995).
²⁵L. Spiess, P. S. Mangat, S. P. Tang, K. M. Schirm, A. J. Freeman, and P. Soukiassian, Surf. Sci. Lett. **289**, L631 (1993).
²⁶B. W. Holland, C. B. Duke, and A. Paton, Surf. Sci. **140**, 269 (1984).
²⁷F. Bechstedt and D. Reichart, Surf. Sci. **202**, 83 (1988).